Journal of Materials Chemistry B

Accepted Manuscript

ROYAL SOCIETY OF CHEMISTRY

www.rsc.org/materialsB

A novel legumain protease-activated micelle cargo enhances anticancer activity and cellular internalization of doxorubicin

Sen Lin[a, b], Fangfang Deng[a], Ping Huang[a], Lingli Li[a,b], Lei Wang[b], Qing Li[b], Ling Chen[c], Hao Chen [a, b*], Kaihui Nan[a, b*]

Abstract Legumain is the only acidic asparaginly-endopeptidase in mammals that is highly up-regulated in tumor tissue and tumor associated cells. In this study, a novel legumain protease-activated micelle was successfully synthesized and prepared loading doxorubicin (DOX). The prepared micelle was exhibited as spherical morphology and possessed a low critical micelle concentration of 1.21×10^{-3} mg/mL with a DOX loading capacity and entrapment efficiency of 4.05% and 60.6% respectively. The release profile of DOX from this micelle formulation was observed as legumain concentration dependent. The micelle encapsulation of DOX highly enhanced the cellular uptake of DOX by tumor cell lines of DAOY, Y79, MCF-7, and MCF-7/DOX. Furthermore, encapsulation of DOX boosts the cytotoxicity against the tumor cells while reducing cytotoxicity against RPE and HEK293 cell. In addition, blank micelles did not exhibit any biological effects on tumor or RPE or HEK293 cell at the concentration range of 0-300 μg/mL, indicating good biocompatibility. The results suggest this micelle formulation has potential applications in sustained drug delivery for legumain up-regulated tumors.

1. Introduction

Doxorubicin (DOX) is widely employed as a chemotherapy agent for many cancers; however it causes substantial risk of systemic toxicity especially cardio-toxicity. The development of nano-scale drug delivery systems seeks to reduce the off-target toxicity and improve the therapy index upon the enhanced permeation and retention (EPR) effect of tumor tissues. Take Doxil (Janssen Biotech), a DOX nano-carrier, as an example, compared to the free DOX, Doxil increases the circulation half-life 100 times concomitant with a reduction of the cardio-toxicity sevenfold[1]. But these improvements were not always significant enough for clinic treatment, such as when Doxil was used as first-line therapy in breast cancer patients[1]. To expand the benefit of these nano-agents, multifunctional nanoparticles were designed and developed upon the pathological features of tumor tissue or its microenvironment such as higher expression of folate receptors[2, 3], lower PH values[4-6], and higher reduction potentials[7, 8], when compared to normal tissues.

Legumain, the only asparaginly-endopeptidase in mammals, is an acidic cysteine protease that specifically cleaves the C-terminal side of the asparagine residue at the P1 position of substrates[9]. It was found to be highly up-regulated in tumor cell and tumor associated macrophages and endothelial cell[10]. It was secreted to tumor micro-environments which lead to tumor progression, angiogenesis, and metastasis. Legumain has a caspase-like structure, with a central six-stranded β-sheet, flanked by five major α-helices[11]. It is initially produced as pro-legumain with a 50-60 kDa molecular weight containing a "pro-domain" on the top of an "activity domain" contributing to activity blocking and enzyme stabilization. The "pro-domain" can be removed by acidic condition (pH3.0-6.0), which induces its asparaginly-endopeptidase activity. The expression of legumain can be induced; and the activity of this enzyme is regulated by stress conditions such as hypoxia, starvation, and low pH values. Legumain only exhibits proteolytic activity under acidic condition (pH3.0-6.0), and is inactivated in physiologic conditions (pH 7.0). In the human colon cancer (HCT116) and human metastatic colon carcinoma (SW620) cell lines, legumain was found to be distributed in the cytosol, lysosome, nuclear, and conditioned culture media[12]. These characteristics make legumain an ideal target for drug treatment or drug delivery system design.

Several strategies concerning overexpression of legumain in tumor tissue were developed for drug delivery. Wu et al.[10] synthesized a legumain-activated pro-drug platform by the introduction of a legumain degradable peptide to DOX via an amide bond formation between the amino group of DOX and the terminal carboxyl group of the peptide substrate, which reduced the side effect of DOX and increased tumoricidal activity. Another pro-drug, linking of legumain substrate peptide with etoposide, was reported to increase its antitumor effect[13].But such strategies that directly link drug to protease

substrate peptide need specific synthesis for each drug and highly depend on the particular molecular structure of the drugs [14], as descripted in Wu's report[10] specially requiring amino groups in drugs to form an amide bond linked pro-drug. Furthermore, this kind of pro-drug could not increase the circulation half-life of drug in human body. Others have developed liposome, chitosan nanoparticles to deliver payload DNA or anti-cancer drugs to target tumor tissue or its micro-environment though grafting a legumain ligand to the surface of nanoparticles[15-19]. These kinds of targeting nanoparticles were also targeted to inactivated pro-legumain which was present both in tumor tissue and normal tissue. A recent published study reported a novel liposome that was coated with a legumain protease-activated cell penetrating peptide which exhibited good targeting efficacy[14]. However, to the best of our knowledge, the legumain protease-activated micelle for drug delivery was not documented previously.

In this study, we designed and synthesized a legumain protease-activated micelle to deliver a payload of DOX by a linkage of hydrophilic polyethylene glycol (PEG) and hydrophobic poly (benzyl glutamate) (PBG) via a legumain specific substrate peptide (PEP). We hypothesize that drug will be released in the site that possesses high legumain activity, thus increasing the target efficacy and anticancer activity. The structure of this copolymer was identified by ^{1}H nuclear magnetic resonance (^{1}H-NMR) and Fourier transforms infrared spectroscopy (FT-IR). This amphiphilic copolymer was self-assembled to form micelles using a dialysis method. The morphology of micelles was observed by high resolution transmission electron microscopy (HR-TEM). The cytotoxicity of free DOX (F-DOX) and encapsulated DOX with micelle against a human retinoblastoma cell line (Y79), a human medulloblastoma cell line (DAOY), a human breast cancer cell line (MCF-7), a DOX resistance human breast cancer cell line (MCF-7/DOX), a human embryonic kidney cell line (HEK293), as well as a human retinal pigment epithelial (RPE) cell were studied.

2. Materials and methods

2.1 Materials

Doxorubicin hydrochloride (DOX•HCl), N,N-Diisopropyl-ethylamine (DIPEA), 2-(7-Aza-1H-benzotriazole-1-yl)-1,1,3,3-tetramethyluronium hexafluorophosphate (HATU), and triisopropylsilane (TIS) were purchased from Aladdin Reagents (Shanghai, China). The legumain tetra-peptide substrate and methoxy amino-poly (ethylene glycol) (mPEG-NH_2, Mw=10000 Da) were provided by KareBay Biochem, Inc. (Ningbo, China). The cell lines used in this study were all sourced from American Type Culture Collection (ATCC) (Rockville, MD, USA), and maintained in Dulbecco's RMPI 1640 medium (Gibco, Invitrogen, Carlsbad, CA) supplemented with 10% fetal bovine serum (Invitrogen, Carlsbad, CA). All the reagents used in the study were analytical pure ones. The deionized water was prepared with a Milli-Q water filtration system (Millipore, Bedford, MA, USA) before being used.

2.2 Synthesis of mPEG-PEP-NH_2

The tetra-peptide (HO-AAN(Trt)L-NH-Fmoc,100 mg) was dissolved in N,N-dimethyl formamide (DMF) and maintained at 0 ℃, and then was introduced to methoxy mPEG-NH_2 (800 mg） by amid bond formation between the amino group of mPEG-NH_2 and carboxyl group of HO-AAN(Trt)L-NH-Fmoc using DIPEA (45 μL) and HATU (50 mg) as the coupling agent. The solution reacted at room temperature for 12 h with stirring. The product was collected after precipitating with diethyl ether then centrifuging at 8000 rpm for 10 min.

2.3 Synthesis of mPEG-PEP-PBG copolymer

The amphiphilic copolymer was synthesized via ring opening polymerization of γ-benzyl-L glutamate N-carboxy anhydride (BLG-NCA) initiated from the terminal amino group of mPEG-PEP-NH_2. Briefly, BLG-NCA (200 mg) was dissolved in dry DMF (5 mL) followed by the addition of 43 mL dehydrated dichloromethane (DCM) and then 1 g of mPEG-PEP-NH_2 was added. The reaction was carried out with stirring at 37 ℃ for 24 hour in a nitrogen stream. The product was harvested via precipitation with diethyl ether, centrifugation and lyophilization in sequence. The resultant powder was re-dissolved in DMF and was dialyzed against distilled water using a MD34 dialysis bag (Solarbio Life Sciences CO., Beijing, China) with a molecular weight cut off of (MWCO) 3500 Da. The resultant copolymer was used to prepare responsive micelle.

In addition, the copolymer without legumain tetra-peptide substrate was synthesized via ring opening polymerization of BLG-NCA initiated from the terminal amino group of mPEG-NH_2 forming amphiphilic diblock copolymer mPEG-PBG. This copolymer was further used to prepare non-legumain responsive micelle.

2.4 Structure characterization of copolymer

The molecular weight was measured by gel permeation chromatography (GPC) using polystyrene with different molecular weights (1270, 3180, 6940, 20000, 52500 Da) as the standard. The analysis was performed using high-performance liquid chromatography (Waters 5215, Milford, MA) equipped with a Styragel HR-2 column (7.8 ×300 mm) , a Styragel HR-3 column (7.8 ×300 mm), and a Styragel HR-4 column (7.8 ×300 mm) coupled with a 2414 refractive index detector and a Breeze GPC workstation. After filtration, 50 μL of the samples were loaded and eluted with tetrahydrofuran at a flow of 1.0 mL/min at 35 ℃. The molecular weights were calculated from an equation based on the elution volume of the standard polystyrene to the log of their molecular weight.

The structure of copolymer was identified by ^{1}H-NMR and FT-IR spectroscopy. ^{1}H-NMR spectra was recorded by a Bruker AC 400 instrument (Rheinstetten, Germany). Samples were dissolved in $CDCl_3$. FT-IR spectra were measured on a Nicolet 5700 FT-IR spectrometer (Thermo Electron, USA). The samples were prepared as KBr tablets.

2.5 Critical micelle concentration (CMC)

The CMC of mPEG-PEP-PBG in deionized water was determined according the method described by Cao et al. [5] using pyrene as a probe. Briefly, 50 μL of a 12 μg/mL pyrene/acetone solution was added into tubes. The acetone was removed under vacuum. The polymer was added into the tubes with different final concentrations (varying from 1×10^{-4} mg/mL to 0.1 mg/mL). The resultant mixture was treated with ultrasonic waves for 4 hours, and further kept away from light

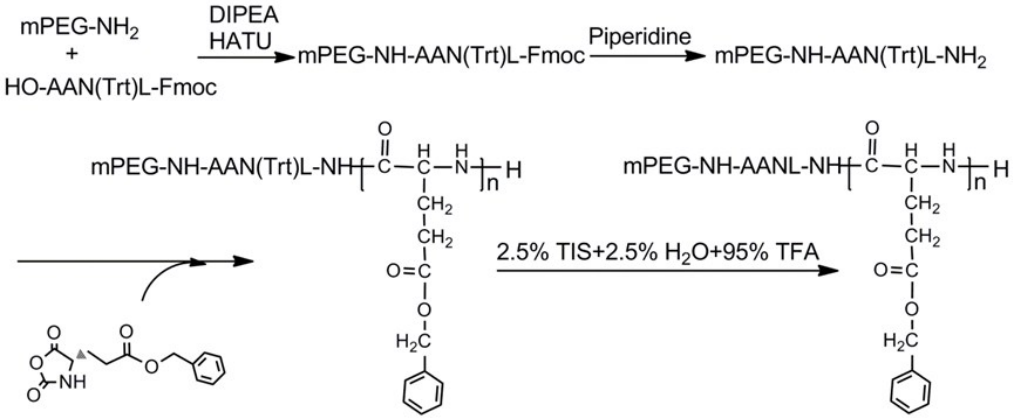

Scheme.1 The synthetic rout of mPEG-PEP-PBG copolymer

overnight. The fluorescence excitation spectra were measured with the emission wavelength of 390 nm and the fluorescence intensity at 338 (I338) and 333 nm (I333) were recorded by an F-4600 fluorescence spectrophotometer (Hitachi Co., Japan). The value I338/I333 was calculated and plotted against the concentration of the copolymer. The CMC was estimated as the cross-point of extrapolating the I_{338}/I_{333} value at low and high copolymer concentrations.

2.6 The stability of micelle

The stability of micelle with the present of fetal bovine serum (FBS) was evaluated in neutral condition (pH 7.0) and acid condition (pH 5.0). Specifically, micelle was mixed with PBS buffer (pH 7.0) or acetate buffer (pH 5.0) containing 45 g/L of FBS and 0.05% (w/v) NaN_3. The final concentrations of micelle in both buffer solutions were 0.05 mg/mL. The mixtures were incubated at 37 ℃ in an orbital shaker at 150 rpm. At given time points, 2 mL of the mixtures were taken out and analyzed using a dynamic light scattering (DLS) size analyzer (Brookhaven Zeta plus instrument).

2.7 Preparation of DOX loaded micelle

The DOX loaded legumain-responsive micelle was acquired with the method described by Boddu et al.[20]. Briefly, DOX•HCl (5 mg) was dissolved in DMSO and then was neutralized with 1.3 eq of triethylamine. After the addition of mPEG-PEP-PBG, the mixture was stirred and ultrasonically treated for 2 h. The resultant mixture was dialyzed for 2 days against distilled water. The micelle powder was harvested after freeze drying and characterized for drug loading capacity (LC), entrapment efficiency (EE), particle size and distribution, as well as morphology. Moreover, the copolymer mPEG-PBG was employed to prepare non-legumain responsive micelle using the same method.

The LC and EE were determined by fluorescence measurement[21]. The lyophilized drug loaded micelles were precisely weighed and dissolved in DMSO. The fluorescence emission wavelengths at 590 nm and excitation wavelengths at 480nm were recorded by an F-4600 spectrophotometer. The amount of DOX was determined by comparing to a calibration curve of DOX in DMSO. The LC and EE were calculated according to the following equations:

$$\text{LC}\ (\%) = \frac{\text{Weight of DOX in the micelles}}{\text{Weight of DOX loaded micelles}} \times 100$$

$$\text{EE}(\%) = \frac{\text{Weight of DOX in the micelles}}{\text{Weight of theDOX feeded}} \times 100$$

The particle size and zeta potentials of micelles were measured using a dynamic light scattering size analyzer. The polydispersity of the particles were also measured. The morphology of the micelles was observed by HR-TEM (Tecnai G2 F20 S-TWIN, FEI). Briefly, small amounts of micelle solution were dropped onto a carbon-coated copper grid and were subjected to TEM analysis after completely drying.

2.8 In vitro drug release profile

The recombined legumain was purchased from Novoprotein Inc. (US) and was activated in a buffer containing 50 mM sodium acetate and 100 mM NaCl (pH=4.0) for 2 h at 37 ℃. Ten milligram of DOX loaded micelle powder was dispersed in 50 mL of a mixture containing 0.1 M of 4-Morpholineethane-sulfonic acid hydrate and 250 mM NaCl (pH 5.0). Subsequently, 2 mL of this solution was introduced into a dialysis bag (MWCO=3500 Da, diameter=0.8 cm) and was immerged into vials containing 3 mL of above mentioned solution. In order to remove the leaked DOX, the vials were pre-treated in a shaker bath at 37 ℃ for 30 min and then dialyzed solution was replaced with fresh solution. Afterwards, 5 μL of legumain (100 ng) was added into the dialysis bag and was cultured under the same conditions. At regular time intervals, 200 μL of solution with released drug was taken out for further analysis and the same volumes of fresh solution were added into the vials. The released DOX was measured with a fluorospectro-photometer (F-4600, Hitachi, Japan) at 485 nm (excitation wavelength) and 595 nm (emission wavelength). All experiments were carried out in triplicates.

2.9 Cellular uptake studies

The cellar uptake ability of legumain responsive micelle encapsulated DOX (LRME-DOX), non-legumain-responsive micelle encapsulated DOX (NRME-DOX), and free DOX (F-

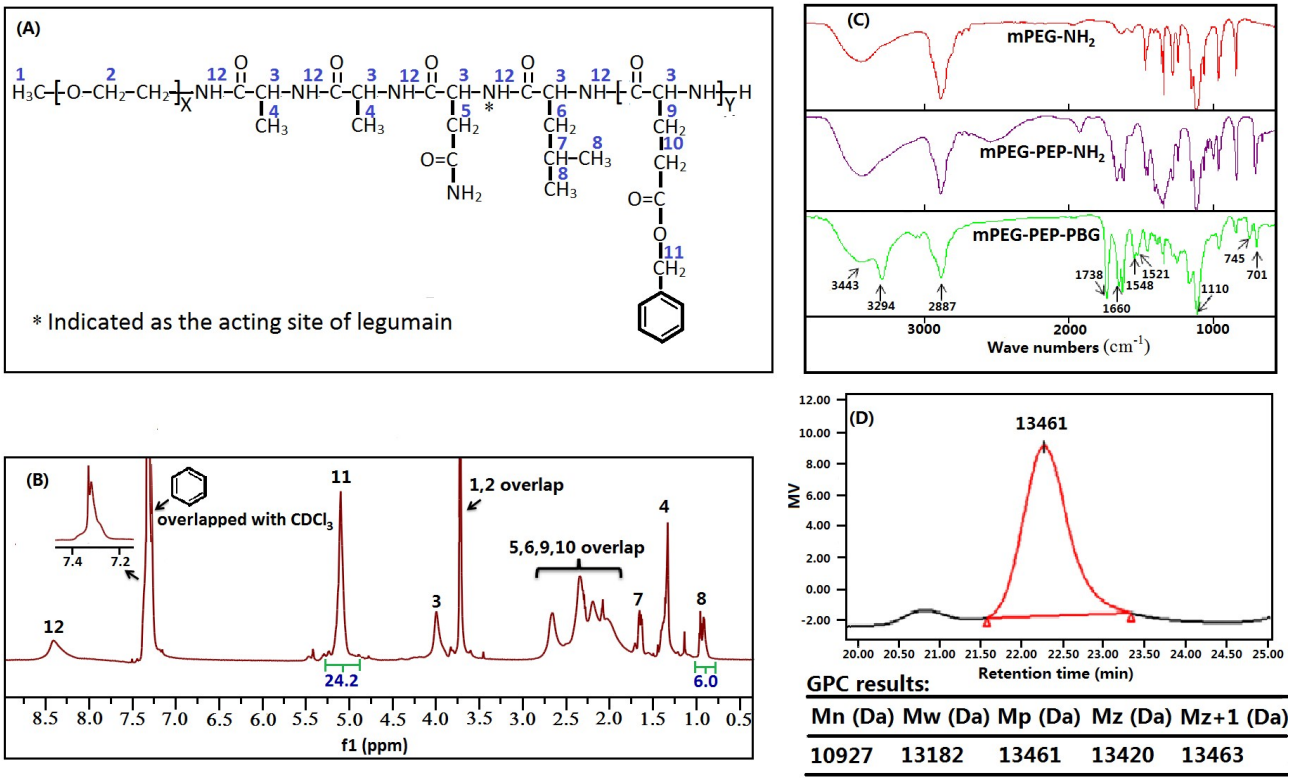

GPC results:

Mn (Da)	Mw (Da)	Mp (Da)	Mz (Da)	Mz+1 (Da)
10927	13182	13461	13420	13463

Fig.1 Characterization of copolymer. Molecular structure (A), 1H-NMR spectra (B), FT-IR spectrum (C), and GPC chromatography of mPEG-PEP-PBG (D).

.

DOX) were measured as described by Tsai et al.[22]. Specifically, 5×10^4 cells were seeded in a 12-well plate and further maintained in RMPI 1640 medium supplemented with 10% FBS at 37 ℃ in a 5% CO_2 incubator for 24 h. The medium was then replaced with fresh medium containing 0.7 μg of F-DOX, or equivalent LRME-DOX, or equivalent NRME-DOX. The cells were cultured at the same conditions for an additional 3 h. The culture medium was removed and the plate was washed with PBS for 3 times. For fluorescence microscopy, 0.2 mL of PBS containing 2.5 μg of fluorescein diacetate (FDA) was added to each well and incubated for 10 min at 37 ℃ in the dark. The fluorescence of DOX (red) and fluorescein (green) can be monitored by excitation at 480 nm (emission at 590 nm) and 495 nm (emission at 535 nm) respectively. The fluorescence images were obtained at 20×magnification using a digital camera (Nikon CO., Japan) equipped with fluorescence accessories. In addition, as Y79 is a suspension cell, it was collected by centrifugation at 1000 rpm for 5 min and re-suspended with PBS (for washing) or FDA-PBS solution (for fluorescence microscopy). It was observed according to the method mentioned above.

The intracellular location of F-DOX and LRME-DOX were compare studied using the method described by Yang et al.[23] with minor modification. In briefly, the cells were seeded in a 6-well plate containing a piece of glass slide in each well and further maintained in culture medium for 24 h. The cells were then incubated with 0.7 μg of F-DOX, or equivalent LRME-DOX for 2 h. The cells were stained with 4',6-diamidino-2-phenylindole (DAPI), then observed and imaged under 63 × magnification using a confocal microscope (TCS SP5, Leica Microsystems, Germany).

To quantitatively study the uptake, 4×10^5 cells were seeded in 6-well plate and cultured for 24 h. Five microgram of F-DOX, or equivalent LRME-DOX, or equivalent NRME-DOX were then added. The cells were cultured for another 2 h. For the adherent cells, the fluorescence intensity were measured on a flow cytometer (Beckman Coulter, CytoFLEX, US) followed with trypsinization, centrifugation, and suspension with PBS. For Y79 cell, it was collected by centrifugation at 1000 rpm for 5 min and then washed twice with PBS. The fluorescence intensity was then measured on a Beckman Coulter.

2.10 Cytotoxicity evaluation

The cytotoxicity of F-DOX, DOX loaded micelles, and blank micelles against Y79, DAOY, MCF-7, MCF-7/DOX, RPE, and HEK293 were evaluated using a Kit-8 assay (CCK-8, Dojindo, Japan). The cells were cultured in RPMI-1640 medium supplemented with fetal bovine serum (10%), and were maintained at 37 ℃ in a humidified atmosphere of 5% CO_2 and 90% relative humidity. After incubation, cells were diluted to 50000 cell/mL and pipetted into 96-well plates (5000 cell/well). Afterward, F-DOX, LRME-DOX, NRME-DOX, or blank micelles were added into each well with designated concentrations. After culturing for 48 h, 10 μL of CCK-8 was pipetted into each well and incubated for an additional 2 h. The cell viability was measured with a plate reader (Apollo LB913, Berthold Technologies GmbH & Co.) at 450 nm. The cell

survival rate was calculated as the percentage of absorbance contributed from treated cells to that of control cells.

2.11 Statistical analysis

The results were present as means ± standard deviations (SD). Data were analyzed by OriginPro 8 (OriginLab CO., Massachusetts, USA). Student t-test was carried out to test any significant differences between the means. Differences between means at the 5% level were considered significant.

3 Results and discussion

3.1 Synthesis and characterization of copolymer

In this study, the legumain-responsive amphiphilic copolymer was formed by linking hydrophilic mPEG-NH_2 and hydrophobic PBG with a legumain-degradable peptide. The synthesis process of this copolymer was present in Scheme 1. The chemical structure of copolymer (Fig.1A) was confirmed by ^{1}H-NMR (Fig.1B) and FT-IR spectroscopy (Fig.1C). The proton shift at 0.93 ppm and 1.38 ppm were contributed by the methyl group of leucine and alanine residue in legumain degradable tetrapetide respectively proving the conjugation between mPEG-NH_2 and peptide (HO-AAN(Trt)L-NH-Fmoc).This result was further supported by the peak at 1660 cm^{-1} on FT-IR spectra of mPEG-PEP-NH_2 which was associated with the C=O stretching of the amide bond in the tetrapetide. The peak at 5.10 ppm on ^{1}H-NMR spectra and new peak at 1738 cm^{-1} on FT-IR spectra of mPGE-PEP-PBG corresponded to the CH_2 group and O=C-O- bond respectively which matched well to the benzyl ester (O=C-O-CH_2-benzyl) indicative of the formation of PBG moiety. This conclusion was further supported by the new peaks at 745 and 701 cm^{-1} on FT-IR spectra of mPEG-PEP-PBG which indicated mono-substitution of benzyl in the copolymer. The Polymerization degree of benzyl glutamate was 12 as calculated by the ratio of integral area of peak at 0.93 ppm (indicating 6 protons) and peak at 5.10 ppm on ^{1}H-NMR spectra.

3.2 The CMC of copolymer

CMC is an important parameter to amphiphilic copolymer micelles especially for the drug delivery application[24]. In this paper, The CMC of mPEG-PEP-PBG was determined by fluorescence spectra using pyrene as the probe. Pyrene is a

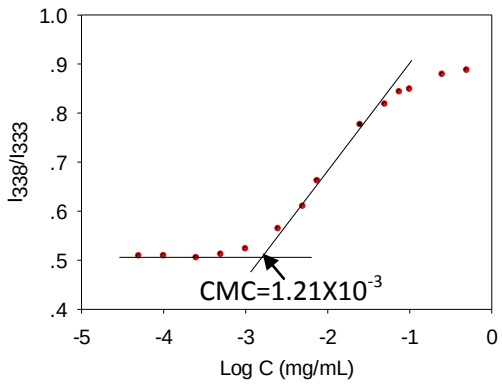

Fig.2 Plot of the fluorescence intensity ratio I338/I333 from pyrene excitation spectra vs. log C (mg/mL) of the mPEG-PEP-PBG co-polymer in distilled water.

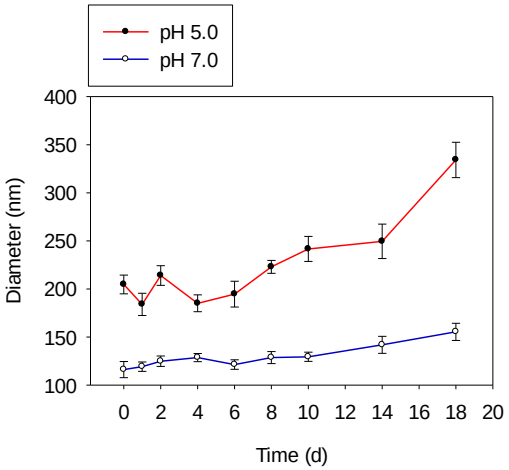

Fig.3 The stability of micelle in neutral condition (pH 7.0) and acidic condition (pH 5.0) with the present of FBS.

strong hydrophobic probe which preferentially distributes in hydrophobic environments, and will be cause a change in its photo-physical properties when entrapped into hydrophobic cores of micelles. The excitation intensity ratio of pyrene at 338 nm and 333 nm (I338/I333) were highly dependent on the fraction ratio of pyrene in hydrophilic to hydrophobic segments. As shown in Fig.2, the I338/I333 sharply increased when concentrations of copolymers were higher than 4.0×10^{-3} mg/mL, indicating the onset of micellization. As derived from Fig.2, the CMC of mPEG-PEP-PBG was determined to be 1.21×10^{-3} mg/mL suggestion good stability of this micelle. This value is by 3 orders of magnitude lower than CMC of odecyltrimethyl-ammonium chloride (an ionic low molecular weight surfactant) [25], and was comparative to other amphiphilic copolymer micelles[3, 5, 26-28]. Such a low CMC value makes it an ideal material for drug delivery, because it can avoid leakage of encapsulated drug from micelles when diluted by body fluid. Previous studies suggested that copolymers with higher hydrophobic Mw/hydrophilic Mw values exhibit lower CMC[24, 30], thus mPEG-PEP-PBG with a lower CMC value can be acquired when lower Mw of mPEG is employed.

3.3 The stability of micelle

The stability of the mPEG-PEP-PBG micelles at 37 ℃ was investigated with the presence of FBS under neutral condition (pH 7.0) and acid condition (pH 5.0). The hydrated diameters of the micelles in buffer were determined via DLS during the period of up to 18 days. As shown in Fig.3, the initial diameter of micelle in acidic condition was about 200 nm. It was stable in first 6 days. The micelle was swelling to 250 nm and 340 nm in 14 and 18 days respectively. In neutral condition, the diameter of micelle was maintained at 120 nm in first 10 days. It was slightly swelling to 135 nm at 14 day and 150 nm at 18 day. These data suggested that this micelle was more stable in neutral condition. The pH value in tumor microenvironment, endosomes, and lysosomes was much lower than that in physiological environment. This suggested that drugs was much easier release from this micelle in tumor tissue than normal tissues, which could enhance targeting efficiency and improving intracellular drug release when the micelle formulation was internalized via endocytosis.

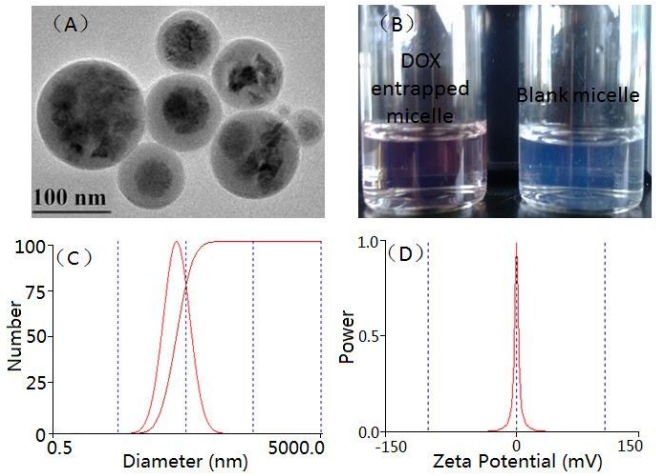

Fig.4 Formation of DOX loaded micelle. (A) HR-TEM image of DOX loaded micelles. (B) Images of blank micelles and DOX entrapped micelles, the copolymer concentration was 0.1 mg/mL, and DOX concentration in the micelle solution was 4.05 μg/mL. (C) Particle size distribution of DOX loaded micelles. (D) Zeta potential of DOX loaded micelles.

3.4 Preparation of DOX loaded micelle

In this study, the DOX encapsulated micelles were prepared via a dialysis method. The loading capacity and entrapment efficiency of the micelles were determined to be 4.05% and 60.6% respectively, which were comparative to many other PEG coated micelles[5]. The morphology of the micelles was observed by HR-TEM (Fig.4A). The micelles present a spherical face with a diameter of approximately 100 nm. The mean size, polydispersity, and zeta potential of the micelles in aqueous solution were measured by dynamic light scattering at 25 ℃ with a micelle concentration of 0.1 mg/mL. The size of the DOX encapsulated micelles were around 115 nm with the size distribution index of 0.206. The zeta potential was determined to be 0 mV (Fig. 3B). Morphology, size, and surface charge can greatly affect cellular uptake and tissue distribution of nanoparticles[30-32]. It was reported that spherical shaped nanoparticle were much easier for cellular uptake than rode shaped nanoparticle by endocytosis[33]. Sizes of 25-50 nm in diameter were proved to be optimal for receptor mediated endocytosis[34], while nanoparticles with a diameter of 100-150 nm were preferred for clathrin-mediated endocytosis[35]. Moreover, nanoparticles with the size of 100-150 nm can be effective as passive targeting drug cargo because of the EPR effect of tumor tissue. In that case, the micelles prepared in this study can be used for drug delivery.

3.5 Drug release profile

The DOX release profile from micelles with or without legumain treatment was studied. As shown in Fig.5, at the first 1 h, 15±2.5% of DOX was released from micelles with the treatment of leguamin while 9.8±3.2% was released at the same time without legumain treatment. Afterwards, up to 70% of DOX was released from the micelle in 15 days indicating this micelle could be applied as a depot for sustained controlled drug release. The release behavior of DOX from micelles with-

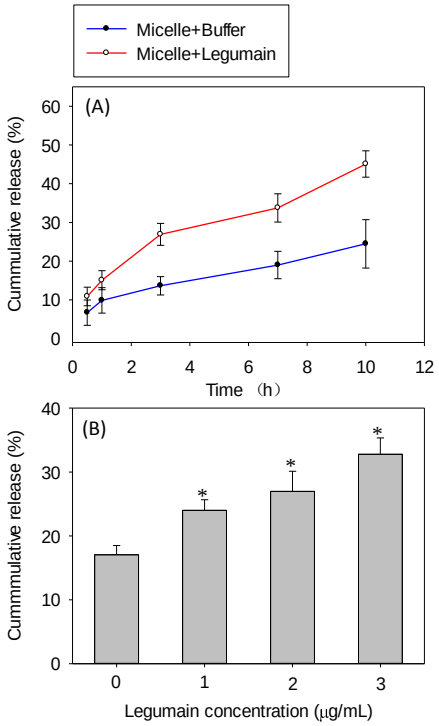

Fig.5 *In vitro* DOX release profile from DOX-encapsulated micelle with the presence of legumain. (A) Time dependence release profile of DOX treated with 2 ug/mL legumain. (B) Concentration dependence release profile of DOX with 5 h treatment. Each point represented mean ± SD of 3 experiments. *P < 0.05 compared with free legumain group (0 ug/mL).

out legumain treatment was comparative to PEG-CA-PCL micelles reported by Jun Gao et al.[5]. The drug release of legumain treated group was much faster than that of legumain un-treated group during the first 10 h. However, there is no significant difference of DOX accumulated in a long term release profile (data not shown). This may because of inactive legumain. Moreover, DOX release from micelles under different legumain concentrations was further studied (Fig.5B). Samples were harvested after treatment with different concentrations of legumain for 5 h and measured with a Hitachi F-4600 fluorescence spectrophotometer. It was found that the release speed of DOX from micelle was legumain concentration dependent. This indicated that the release profile of such micelles were indeed legumain modulated.

3.6 Cellular uptake

The cellular uptake of F-DOX, LRME-DOX, and NRME-DOX were monitored by a fluorescence microscopy with FDA staining. DOX itself can produce red fluorescent at the excitation wave length around 480 nm (Fig.6). While, FDA is non-fluorescent hydrophobic fluorescein derivative and it only exhibits green fluorescent in intra of living cell where possessed esterases to hydrolyze the ester groups of FDA that produced the fluorescent fluorescein[36]. The yellow dots in the merged images represent the DOX entrapped into live cells. For DAOY, Y79, and MCF-7/DOX cell line, it was found that the color on the emerged image of micelle encapsulation DOX treated group (NRME-DOX and LRME-DOX) was much darker than that of F-DOX treated group, indicating that micelle

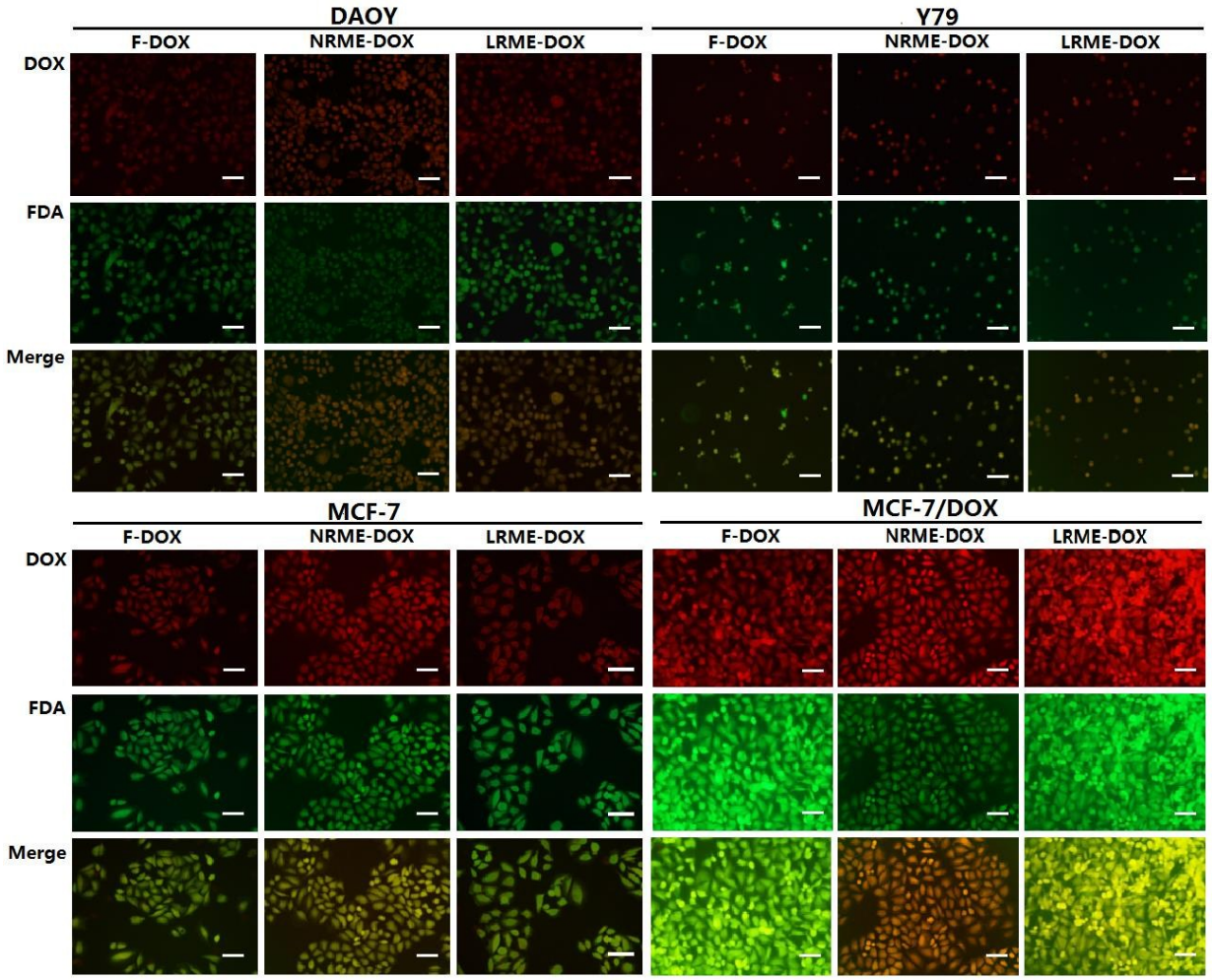

Fig.6 Fluorescence microscope images of DAOY, Y79, MCF-7, and MCF-7/DOX cell lines, after incubating with F-DOX or ME-DOX and staining with FDA. Scale bar: 10 μm.

encapsulation improved the internalization of DOX for these cells. For MCF-7 cell line, there was no significant difference between the two groups with naked eye. In order to quantify cellular uptake of micelles by these tumor cells, samples were further measured by flow cytometry and the results were analyzed with the Cytexpert work station. For the DAOY cell line, 94.1% of the cells were DOX positive when incubated with micelle encapsulated DOX for 2 h, compare to 79.8% of DOX positive cells observed when cultured with equal concentrations of F-DOX under the same conditions (Fig.7A). This increase was also found for the Y79 cell line (increased from 51.1% to 93.1%). Moreover, a dramatic increase for mean fluorescence intensity (Fig.7B) for the Y79 cell line was observed with the treatment of micelle encapsulated DOX (NRME-DOX and LRME-DOX), which indicated that micelle encapsulation of DOX not only increased the population of DOX positive cell but also enhanced the DOX internalization of single cells (Fig.7 B). With F-DOX treatment, the DOX positive population of MCF-7 cells (57.5%) was much bigger then MCF-7/DOX cells (28.5%). This is reasonable because MCF-7/DOX as a DOX resistance cell line can expel DOX via its overexpressed ATP-binding cassette (ABC) transporters (e.g. P-glycoprotein and multidrug resistance associated-protein 1) thus maintaining intracellular DOX concentrations at a low level[37, 38]. Micelle capsulation of DOX greatly increased cellular uptake of MCF-7/DOX cells (both for the population and single cells). Moreover, an increased DOX positive cell population as well as a higher average fluorescent intensity was also observed for the MCF-7 cell line. These results were in some degree contradicted with the observation of the fluorescence microscope (Fig.6) which indicated no significant difference between the micelle encapsulated DOX (NRME-DOX and LRME-DOX) treated group and F-DOX treated group. In order to make the experiments comparative, all of the images (Fig.6) were taken with the same conditions with the exposure time for DOX and FDA fluorescence fixed at 600 and 20 milli-seconds respectively. This can be caused by underexposure of images for MCF-7 cell, thus covering the differences of these groups, as the light exposure time can greatly affect the resultant fluorescent images. In addition, no significant difference of the cellular uptake between NRME-DOX and LRME-DOX were observed.

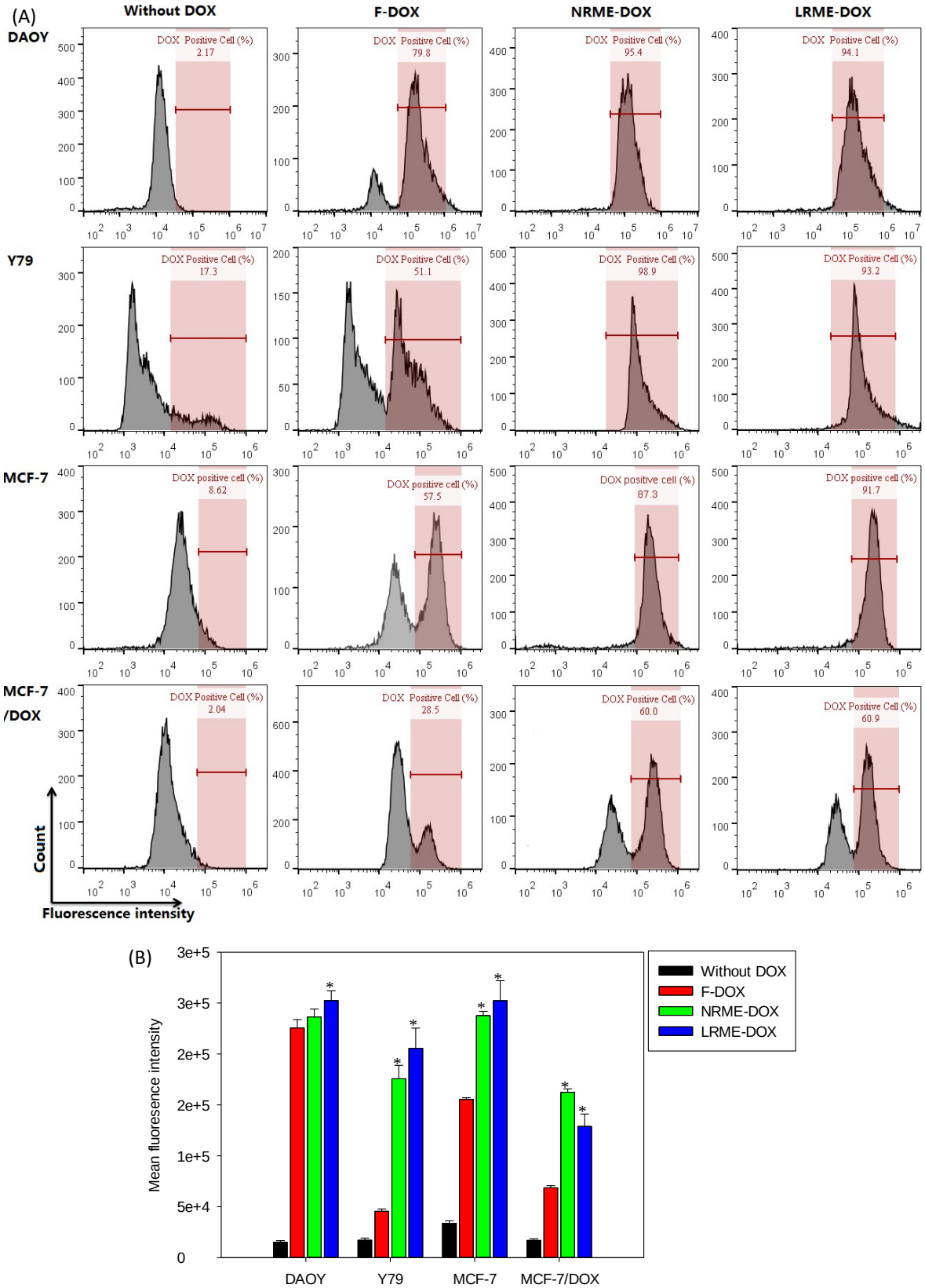

Fig.7 Flow cytometer evaluation of cellular uptake. (A) The representative diagrams of different groups. The data in each diagram are the percentage of DOX positive cells given by flow cytometry software. (B) The average fluorescence intensity of cells given by flow cytometry software. Each point represented mean ± SD of 3 experiments. *P < 0.05 compared with "F-DOX" group.

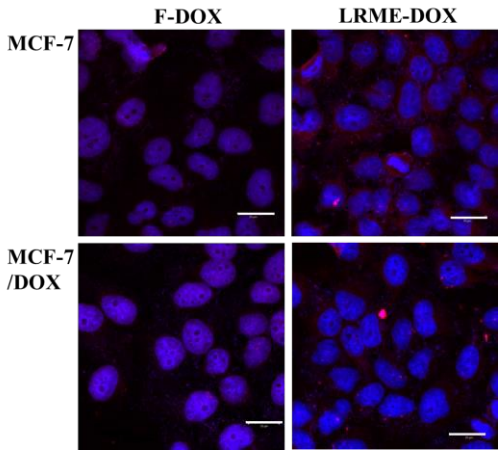

Fig.8 The merged confocal microscopic images of the intracellular distribution of DOX (red) in MCF-7 or MCF-7/DOX with DAPI (blue) staining. Scale bar: 20 μm.

The intracellular distributions of DOX in MCF-7 and MCF-7/DOX cells after internalization were observed with a confocal laser scanning microscope (Fig.8). In the F-DOX treatment group, most of the drug was located uniformly with DAPI, which indicated that the F-DOX was accumulated in the nuclei of MCF-7 and MCF-7/DOX cells at 2 h. Similar results were previously observed by Yang et al.[23] when MDA-MB-231-GFP-fLuc cells were employed. In the LRME-DOX treatment group, DOX was distributed both in cytoplasm and nucleus after 2 h incubation, possibly because LRME-DOX was firstly distributed in the endosomes after endocytosis, then released in cytoplasm, and diffused into nucleus afterward.

3.7 The cytotoxicity evaluation

In the present study, the cytotoxicity of F-DOX, LRME-DOX, and NRME-DOX against DAOY, Y79, MCF-7, MCF-7/DOX, RPE cell and HEK293 cell were studied in parallel. The results are presented in Fig.9 and Fig.10. They were observed as concentration depended. As shown in Fig.9A, the IC50 value of F-DOX against DAOY was determined to be 1.3 μg/mL. The inhibition effect of DOX against the DAOY cell line was in some cases contradicted in the available literatures that some reported cell viability was 43% at 0.1 mg/mL of DOX[38] while others determined to be 41.5% at the concentration of 0.01 μM (0.0058 μg/mL)[39]. This may be because of different origins of the cells and different analysis methods adopted. The encapsulation of legumain responsive micelle of DOX significantly enhanced the anti-proliferation of DAOY at the concentrations of 0.43, 0.56, and 0.7 μg/mL. These enhancements could be contributed by the promoted cellular uptake of DOX with micelle encapsulation. The trends of Y79 cell lines were similar to DAOY, but it was much more sensitive to DOX than DAOY (Fig.9B). However, the difference of IC50 value of F-DOX and LRME-DOX to Y79 was not significant (about 0.4 μg/mL). As the MCF-7/DOX is a DOX resistant cell line, it was treated with a DOX concentration ten times that of MCF-7 (a non-drug resistant cell line). As shown in Fig.9C and D, the IC50 value of F-DOX for MCF-7 and MCF-7/DOX was about 0.9 and 13 μg/mL

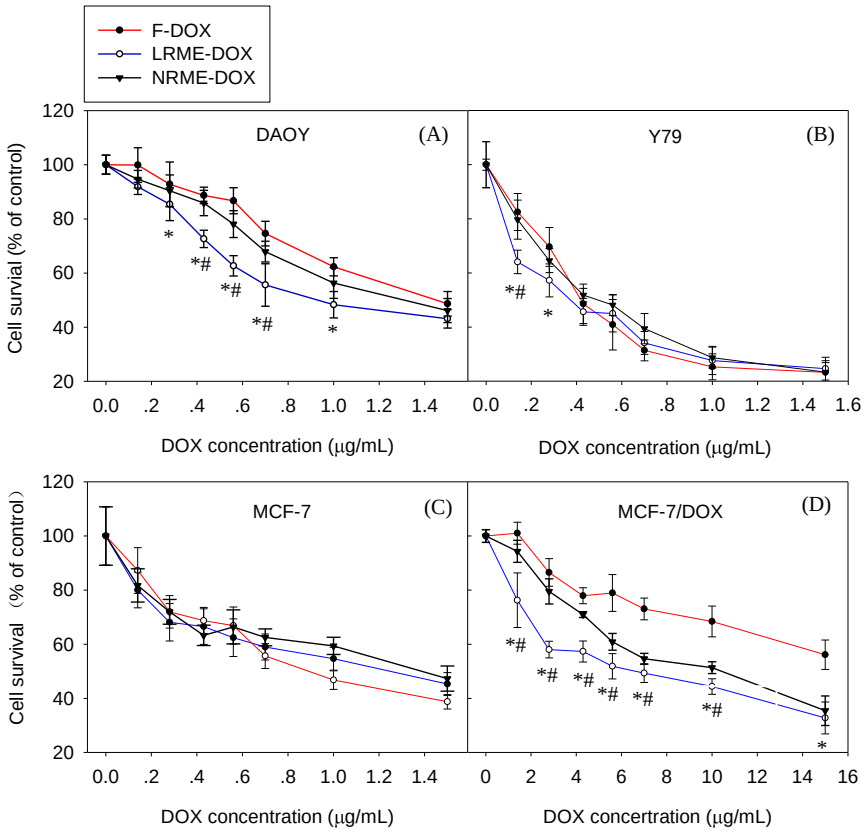

Fig.9 Cytotoxicity of F-DOX and ME-DOX against DAOY (A), Y79 (B), MCF-7 (C), and MCF-7/DOX (D) cell lines. Each point represents the mean ± SD of 5 experiments. *P < 0.05 compared at each concentration of F-DOX and LRME-DOX, # P < 0.05 compared at each concentration of NRME-DOX and LRME-DOX.

respectively. These values matched well with the previous reports[3, 40]. When compared to F-DOX, encapsulation of DOX enhanced cytotoxicity against MCF-7 at low concentrations while reducing such effects at high concentrations (up to 0.7 μg/mL). But these differences were not significant when examined by a Students T test. Furthermore, encapsulation of DOX dramatically enhanced its cytotoxicity against the MCF-7/DOX cell line.

The cytotoxicity of LRME-DOX and NRME-DOX were comparatively studied. The results suggested that LRME-DOX possessed higher inhibition effect against DAOY and MCF-7/DOX cell lines than NRME-DOX. However, the cytotoxicity of LRME-DOX and NRME-DOX against MCF-7 were not significantly different. Moreover, Y79 cell line showed more sensitive to LRME-DOX than NRME-DOX at low concentration (0.14 μg/mL). And no significant difference can be observed at the concentration above 0.3 μg/mL.

In order to evaluate the cytotoxicity of micelle encapsulated DOX against non-cancer cells, RPE and HEK293 cell lines were subjected to F-DOX, LRME-DOX, and NRME-DOX treatments (Fig.10). The results suggested that RPE cells were highly sensitive to F-DOX (IC50=0.14 μg/mL). However, micelle encapsulation of DOX dramatically reduced its cytotoxicity against RPE (IC50 was increased to 0.5 μg/mL). Reduced cytotoxicity of micelle encapsulation DOX (LRME-DOX and NRME-DOX) against HEK293 cell lines was also observed. Moreover, no significant difference of the cytotoxicity of LRME-DOX and NRME-DOX against RPE and HEK293 was observed. In additionally, no significant cytotoxicity of blank micelles against HEK293, DAOY, Y79, MCF-7, and MCF-7/DOX cell lines at the concentration ranges of 0 to 300 μg/mL was observed (Fig.11). However, about 15%

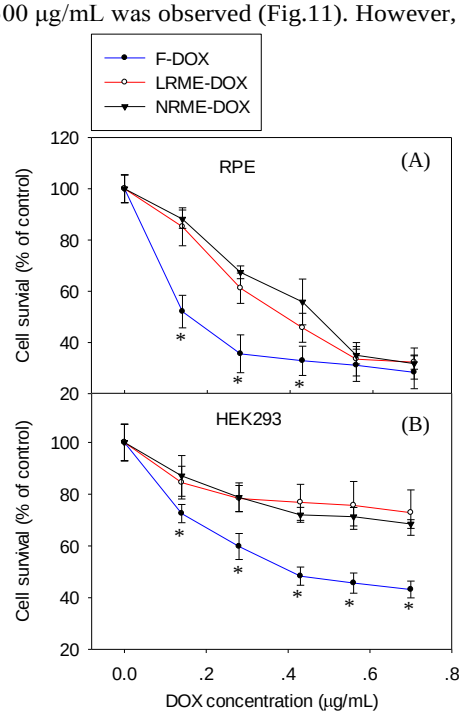

Fig.10 Cytotoxicity of F-DOX and micelle encapsulated DOX (LRME-DOX and NRME-DOX) against RPE (A), and HEK293 (B) cell lines. Each point represents mean ± SD of 5 experiments. *P < 0.05 compared at each concentration of F-DOX and LRME-DOX.

of growth inhibition was found for RPE cells at the concentration of 300 μg/mL blank micelle.

Medulloblastoma is the most common malignant brain tumor in children with poor prognosis, while retinoblastoma is the most common pediatric ocular malignant tumor. Breast cancer is the most common cancer among women that account for one in ten of all new cancers diagnosed worldwide each year[41]. Surgery flowed by chemotherapy is the general treatment for these diseases. However, most chemotherapy agents such as doxorubicin, cisplatin, and bleomycine carry substantial side effects. Moreover, DOX can induce phosphorylation of Akt at Ser473 and phosphorylation of the S6 protein at Ser240/Ser244, activating the PI3K/Akt pathway, which reduces the sensitivity of tumor cells to the chemotherapy agents that cause cancer treatment failures[42]. Cancer cells could overexpress ABC transporters increasing efflux of abroad class of drugs, thus further resulting in multi-drug resistance. Nanoparticles with drug payload are internalized though endocytosis thus could avoid the exclusion of the ABC transporters and increase intracellular drug concentration[43, 44]. This study demonstrated that micelles encapsulation of DOX could enhance the internalization of drug both in DOX resistance cancer cell and non-DOX resistance cancer cell lines. It was reported that nanoparticles with size of 100-150 nm were endocytosed in a clathrin-mediated manner[35]. In tumor cells, a mutation of the p53 and Rcs genes strongly improved clathrin-depended endocytosis[45], thus greatly enhancing the internalization of micelles encapsulation DOX.

The encapsulation of DOX with the designed micelle (LRME-DOX and NRME-DOX) significantly enhanced the cytotoxicity against DAOY and MCF-7/DOX. This could be ascribed to improving internalization of micelle encapsulated DOX. Such effects were further improved with treatment of LRME-DOX (compared with NRME-DOX). It was reported that legumain was highly up-regulated in metastasis breast cancer cell which developed drug resistance[14]. This could increase the release speed of DOX in MCF-7/DOX cell, which possibly caused the improvement of cytotoxicity of LRME-DOX against MCF-7/DOX. Although the encapsulation of DOX did not significantly improve its cytotoxicity against Y79 cell line, it did reduce the cytotoxicity of DOX to normal RPE cells which were very sensitive to DOX. The IC50 value of LRME-DOX against Y79 cells was determined to be 0.5 μg/mL which was close to that of RPE cells (0.4 μg/mL). However, taking account of the EPR effect in solid tumor tissue, the DOX will be mainly distributed in tumor tissue. Furthermore, due to the fact that legumain is up-regulated in tumor tissue[14] and that the micelles were designated to be legumain activated cargo, cancer cells are able to disassemble the DOX loaded vesicles and release the DOX. This process increases the targeting efficacy to tumor tissues.

4 Conclusions

In conclusion, we have successfully constructed a novel legumain protease-activated micelle cargo. The *in vitro* release profile under legumain treatment suggested it was legumain modulated. The encapsulation of DOX with this micelle significantly enhanced the cytotoxicity to several tumor cell lines while reducing the cytotoxicity to normal cell lines.

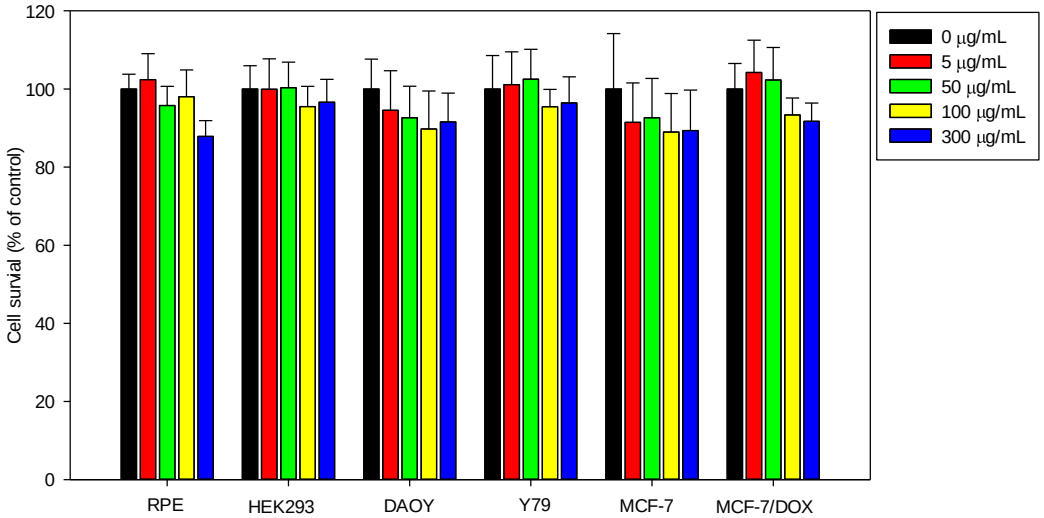

Fig.11 Cytotoxicity of blank micelles against normal cells and tumor cells. Each bar represents mean ± SD from 5 experiments.

This could be ascribed to the enhanced clathrin-mediated endocytosis of this kind of micelle in tumor cells. The novel DOX cargo is expected to have potential applications on sustained drug delivery for the legumain up-regulated tumors such as retinoblastoma, breast cancer and so on.

Acknowledgements

We want to thank Ms. Laura Conner for proofreading of this manuscript. This work was funded by the Natural Science Foundation of Zhejiang Province (No. LQ15H120003, LY12H12005, and LQ14C100003), Science and Technology Planning Project of Wenzhou City (No.Y20140146), and the International Scientific & Technological Cooperation Projects (No.2012DFB30020).

Notes and references

[a] School of Ophthalmology & Optometry and Eye Hospital, Wenzhou Medical University, Wenzhou, 325027, China.
[b] Wenzhou Institute of Biomaterials and Engineering (in preparation), Chinese academy of Science, Wenzhou, 325000, China
[c] Department of emergency surgery, the Second Affiliated Hospital of Anhui Medical University, Hefei, 230022, China
*Corresponding authors: E-mails: nankh@163.com (Kahui Nan) ; Chenhao823@mail.eye.ac.cn (Hao Chen); Fax: +86 577 88833805

1. M. E. R. O'Brien, N. Wigler, M. Inbar, R. Rosso, E. Grischke, A. Santoro, R. Catane, D. G. Kieback, P. Tomczak, S. P. Ackland, F. Orlandi, L. Mellars, L. Alland and C. *Tendler, Ann Oncol*, 2004, **15**, 440.
2. K. Wei, X. M. Peng and F. Zou, *Int J Pharm*, 2014, **464**, 225.
3. L. Y. Qiu, L. Yan, L. Zhang, Y. M. Jin and Q. H. Zhao, *Int J Pharm*, 2013, **456**, 315.
4. G. Thoorens, F. Krier, B. Leclercq, B. Carlin and B. Evrard, *Int J Pharm*, 2014, **473**, 64.
5. J. Cao, T. Su, L. Zhang, R. Liu, G. Wang, B. He and Z. Gu, *Int J Pharm*, 2014, **471**, 28.
6. Q. Duan, Y. Cao, Y. Li, X. Hu, T. Xiao, C. Lin, Y. Pan and L. Wang, *J Am Chem Soc*, 2013, **135**, 10542.
7. W. Cao, Y. Gu, M. Meineck, T. Li and H. Xu, J Am Chem Soc, 2014.
8. S. Cerritelli, D. Velluto and J. A. Hubbell, *Biomacromolecules*, 2007, **8**, 1966.
9. E. Dall and H. Brandstetter, *Acta Crystallogr F*, 2012, **68**, 24.
10. W. Wu, Y. Luo, C. Sun, Y. Liu, P. Kuo, J. Varga, R. Xiang, R. Reisfeld, K. D. Janda, T. S. Edgington and C. Liu, *Cancer Res*, 2006, **66**, 970.
11. E. Dall and H. Brandstetter, *P Natl Sci USA*, 2013, **110**, 10940.
12. M. H. Haugen, H. T. Johansen, S. J. Pettersen, R. Solberg, K. Brix, K. Flatmark and G. M. Maelandsmo, *Plos One*, 2013, **8**, e52980.
13. L. Stern, R. Perry, P. Ofek, A. Many, D. Shabat and R. Satchi-Fainaro, *Bioconjugate Chem*, 2009, **20**, 500.
14. Z. Liu, M. Xiong, J. Gong, Y. Zhang, N. Bai, Y. Luo, L. Li, Y. Wei, Y. Liu, X. Tan and R. Xiang, *Nat Commun*, 2014, 5.
15. D. Liao, Z. Liu, W. J. Wrasidlo, Y. Luo, G. Nguyen, T. Chen, R. Xiang and R. A. Reisfeld, *Cancer Res*, 2011, **71**, 5688.
16. D. Liao, Z. Liu, W. Wrasidlo, T. Chen, Y. Luo, R. Xiang and R. A. Reisfeld, *Nanomed Nanotechnol*, 2011, **7**, 665.
17. X. Zhang, W. Tian, X. Cai, X. Wang, W. Dang, H. Tang, H. Cao, Lin Wang and T. Chen, *Plos One*, 2013, **8**.
18. Z. Liu, D. Lv, S. Liu, J. Gong, D. Wang, M. Xiong, X. Chen, R. Xiang and X. Tan, *Plos One*, 2013, **8**, e60190.
19. Y. Liu, K. M. Bajjuri, C. Liu and S. C. Sinha, *Mol Pharm*, 2012, **9**, 168.
20. S. H. Boddu, J. Jwala, M. R. Chowdhury and A. K. Mitra, *J Ocul Pharmacol TH*, 2010, **26**, 459.
21. Y. Ma, Z. Dai, Z. Zha, Y. Gao and X. Yue, *Biomaterials*, 2011, **32**, 9300.
22. S. P. Tsai, C. Y. Hsieh, C. Y. Hsieh, D. M. Wang, L. L. H. Huang, J. Y. Lai and H. J. Hsieh, *J Appl Polym Sci*, 2007, **105**, 1774.
23. Y. Du, W. Ren, Y. Li, Q. Zhang, L. Zeng, C. Chi, A. Wu and J. Tian, *J Mater Chem B*, 2015, **3**, 1518-1528.
24. X. H. Wang, Q. Tian, W. Wang, C. N. Zhang, P. Wang and Z. Yuan, *J. Mater. Sci.-Mater. Med.*, 2012, 23, 1663.
25. F. M. Menger, *Accounts Chem Res*, 1979, **12**, 111.
26. S. M. Garg, X.-B. Xiong, C. Lu and A. Lavasanifar, *Macromolecules*, 2011, **44**, 2058.

27. Y. Xue, X. Tang, J. Huang, X. Zhang, J. Yu, Y. Zhang and S. Gui, *Colloid Surface B*, 2011, **85**, 280.
28. J. Zhu, Z. Zhou, C. Yang, D. Kong, Y. Wan and Z. Wang, *J Biomed Mater Res A*, 2011, **97A**, 498.
29. Z. Zhang, Q. Qu, J. Li and S. Zhou, *Macromol. Biosci.*, 2013, **13**, 789.
30. F. Yuan, M. Dellian, D. Fukumura, M. Leunig, D. A. Berk, V. P. Torchilin and R. K. Jain, *Cancer Res*, 1995, **55**, 3752.
31. M. Dellian, F. Yuan, V. Trubetskoy, V. Torchilin and R. Jain, *Brit J Cancer*, 2000, **82**, 1513.
32. O. Harush-Frenkel, N. Debotton, S. Benita and Y. Altschuler, *Biochem Bioph Res Co*, 2007, **353**, 26.
33. B. D. Chithrani, A. A. Ghazani and W. C. W. Chan, *Nano Lett*, 2006, **6**, 662.
34. Y. Li, M. Kröger and W. K. Liu, *Biomaterials*, 2014, **35**, 8467.
35. W. Jiang, Y. S. KimBetty, J. T. Rutka and C. W. ChanWarren, *Nat Nano*, 2008, **3**, 145.
36. C. Lv, Z. Wang, P. Wang and X. Tang, *Langmuir*, 2012, **28**, 9387.
37. E. S. Lee, K. Na and Y. H. Bae, *J Control Release*, 2005, **103**, 405.
38. R. Martínez-Zaguilán, N. Raghunand, R. M. Lynch, W. Bellamy, G. M. Martinez, B. Rojas, D. Smith, W. S. Dalton and R. J. Gillies, *Biochem Pharmacol*, 1999, **57**, 1037.
39. T. Zuzak, L. Rist, J. Eggenschwiler, M. Grotzer and A. Viviani, *Anticancer Res*, 2006, **26**, 3485.
40. Y.-H. Lin, J.-H. Chiu, W.-S. Tseng, T.-T. Wong, S.-H. Chiou and S.-H. Yen, *Cancer Chemoth Pharm*, 2006, **57**, 525.
41. J. Ferlay, C. Héry, P. Autier and R. Sankaranarayanan, in Breast Cancer Epidemiology, Springer, 2010, pp. 1-19.
42. A. S. Guerreiro, S. Fattet, B. Fischer, T. Shalaby, S. P. Jackson, S. M. Schoenwaelder, M. A. Grotzer, O. Delattre and A. Arcaro, *Clin Cancer Res*, 2008, **14**, 6761.
43 Y. Sun, X.-Y. Chen, Y.-J. Zhu, P.-F. Liu, M.-J. Zhu and Y.-R. Duan, *J Mater Chem*, 2012, 22, 5128
44 W. Tian, J. Liu, Y. Guo, Y. Shen, D. Zhou and S. Guo, *J Mater Chem B*, 2015, **3**, 1204.
45. I. Mellman and Y. Yarden, *CSH Perspect Biol*, 2013, **5**, a016949.

A novel legumain-responsive micelle was prepared to encapsulate doxorubicin, which increased cellular uptake and anticancer activity of doxorubicin.